MODAL BASED EXPERIMENTAL VIBRO-ACOUSTIC ANALYSIS OF SANDWICH PANELS

Stephen A. Hambric[1], John B. Fahnline[1], Robert L. Campbell[1], Micah R. Shepherd[1], and Stephen C. Conlon[1]

[1]Applied Research Lab, Penn State University
PO Box 30, State College, Pennsylvania, 16804, USA
Email: hambricacoustics@gmail.com

ABSTRACT

Experimental modal analysis techniques are used to compute conductance, vibration energy, and damping loss factors of a stiff lightweight sandwich panel. The panel, constructed from honeycomb core and carbon fiber face sheets, was tested with a shaker, force hammer, and surface-mounted accelerometers. The extracted modal parameters are used to reconstruct panel conductances and surface vibration frequency response functions, filtering out measurement error effects. The modal parameters are also used to exactly compute vibrational energies, even for structures with spatially inhomogeneous mass distribution. The modal energies are confirmed by comparing loss factors inferred using the Power Injection Method (PIM) to those measured directly from the modal analysis, and from decay-based measurements. Finally, radiation damping is computed using an acoustic boundary element (BE) model applied to the measured vibration fields. The radiation damping peak near the panel critical frequency matches the total measured damping nearly exactly, and may be subtracted from the total damping to infer in-vacuo structural damping.

1 INTRODUCTION

The vibro-acoustic properties of panels have been investigated by many authors. Conductance is used to estimate power input to a panel by an external forcing function. Vibration energy is used to estimate mean vibration response of a structure. Total damping is either measured directly, or inferred applying the conductance and energies to the power injection method (PIM). All of these quantities are useful as inputs to Statistical Energy Analysis (SEA) models of interconnected structures and acoustic spaces.

It is common to use a few randomly-spaced excitation and response points to estimate the spatially-averaged energy and conductance for a panel. This works well for homogenous panels (where the density and thickness do not change with location). However, inhomogeneous panels with variable thicknesses or with added structural elements may not be quantified properly with only a few measurement locations. Also, stiff and lightweight sandwich panels have low critical frequencies, and are often strongly damped by sound radiation, which can make determining in-vacuo structural damping difficult.

Experimental modal analysis methods may be used to determine higher fidelity energy and conductance estimates. In this paper, we use parameters extracted from experimental modal analysis data to compute accurate panel energies for spatially non-homogeneous panels using modal reconstruction. The reconstruction approach filters out most errors due to experimental uncertainty. Also, frequency response functions (FRFs) over a dense modal analysis grid are input to an acoustic BE model to compute sound radiation, and thereby radiation loss factors. The radiation loss factors may be subtracted from total damping measurements to infer in-vacuo structural damping.

2 SANDWICH PANEL

A 2.13 m (7 ft) x 1.22 m (4 ft) sandwich panel is shown in Figure 1, and was constructed from 2.54 cm (1 inch) thick Hexcel honeycomb core and carbon-fiber facesheets. Each facesheet is a quasi-isotropic layup of eight plies of 5HSW (5-harness satin weave). The panel ends are reinforced with 0.15 m long facesheet 'doublers', where the facesheet thicknesses are doubled. Table 1 includes the main dimensions and material properties. The panel has been tested and described previously in [1] and [2], which discuss structure-borne power transmission coefficients and coupling loss factors between two panels connected along the width. [1] and [2] also provide a discussion of sandwich panel flexural wavespeeds, conductances, and other quantities.

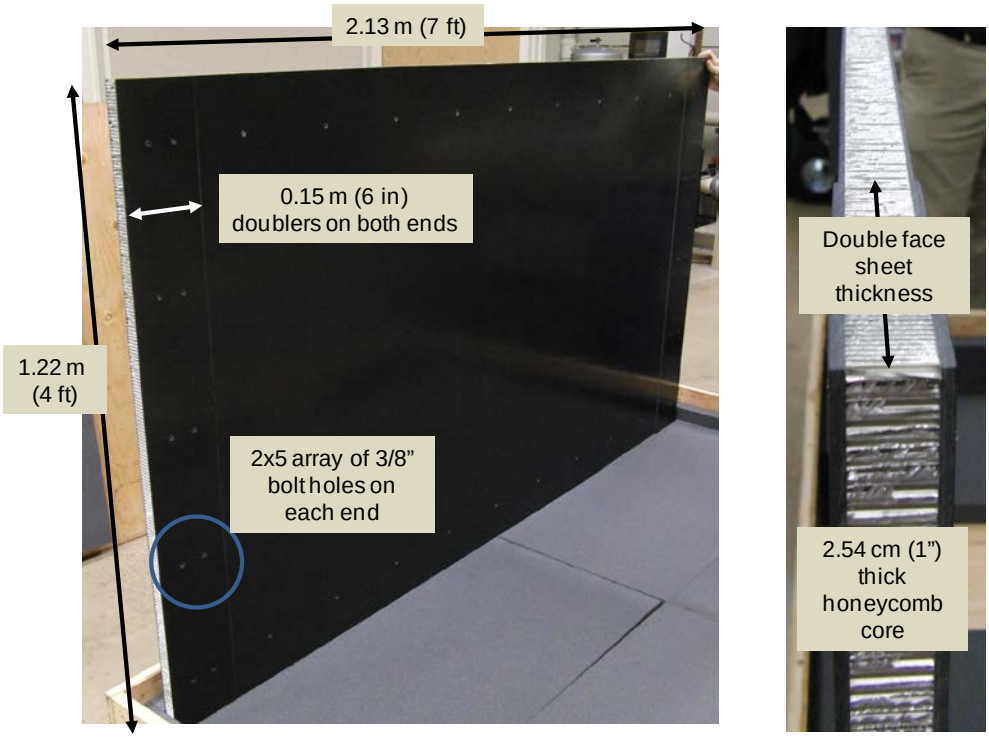

Figure 1: Sandwich panel.

	Length (m)	Width (m)	Young's Modulus (Pa)	Poisson's ratio	Shear Modulus (Pa)	Density (kg/m^3)	Thickness (mm)	Mass (kg)
Facesheets	2.13	1.22	4.76E10	0.30		1603	2.30	19.2
Core	2.13	1.22			5.88E8	130	25.4	8.6
End doublers	0.305	1.22				1603	2.30	2.7
Total/effective	**2.13**	**1.22**				**399**	**34.6**	**30.5**

Table 1: Sandwich panel properties.

3 EXPERIMENTAL AND THEORETICAL APPROACHES

3.1 Measurement procedures

The panel was suspended with soft bungee cords from a large gantry. Two types of measurements were conducted: experimental modal analyses using instrumented force impact hammers and accelerometers, and shaker driven vibrations using a shaker, impedance head, and accelerometers.

For one set of measurements, an electromagnetic shaker (Wilcoxon F3, 25-10,000 Hz usable range, approximately 3 N peak force) was suspended from bungee cords attached to a frame, and mounted to the panel surface via a long stinger and an impedance head (PCB Piezotronics Model 288D01, 99.4 mV/g acceleration sensitivity, 22.6 mV/N force sensitivity) and stud. The impedance head was used to measure both the force applied to the panel, and the resulting panel acceleration. For the modal set of measurements, the panel was driven with an instrumented impulse hammer (PCB model 086C01, 11.2 mV/N sensitivity, up to 440 N peak force). Accelerometers (PCB model 352C66 with nominal 100 mV/g sensitivity and 0.5 to 10 kHz frequency range, 2 gram mass) mounted to the panel and connected to an amplifier (Crown model 288D01) were used to measure normal accelerations for both the shaker-driven and hammer-driven tests. The effects of mass loading of the accelerometers and the impedance head/shaker mass were found to be negligible for frequencies up to 5 kHz.

Measurements were taken at six randomly oriented shaker/hammer input locations. The combination of force and velocity measured with the impedance head may be used to compute the power input per unit force[2], or the conductance:

$$\frac{P_{in}}{\overline{F}^2} = \mathrm{Re}\{Y\} = G\,, \tag{1}$$

where Y is the drive point mobility. The conductance may be averaged over the input locations to compute a surface-averaged quantity. The panel drive point mobility functions are computed from the impedance head measurements as

$$Y = \frac{1}{j\omega} H\,, \tag{2}$$

where

$H = \dfrac{\hat{G}_{fa}}{\hat{G}_{ff}}$ = the measured force – acceleration Frequency Response Function (FRF),

$\hat{G}_{fa}$ = the measured force-acceleration cross-spectrum, and

$\hat{G}_{ff}$ = the measured force autospectrum.

When measuring mobilities with instrumented force hammers, care must be taken since the hammer cannot strike the reference accelerometers directly. The drive point mobilities (and conductances) are therefore averaged over multiple hammer blows, arranged in a tight circle around the accelerometers. For this study, we twice struck the panels in circles subdivided into 45 degree increments (eight drives around the circle) for a total of 16 averages for each drive point mobility.

3.2 Modal parameters

The goal of any modal analysis is to extract eigenvalues (resonance frequencies), eigenvectors (mode shapes), and other modal parameters (modal mass, modal loss factor) from a set of force to vibration FRFs. Once a series of FRFs has been measured, we employ the complex mode indicator function (CMIF) technique developed at the University of Cincinnati to extract modal parameters. The CMIF technique relies heavily on the singular value decomposition (SVD) to help separate the modes before the modal identification process begins [3]-[6].

The implementation within the ARL/Penn State's modal analysis software [7] follows the same basic steps as the original CMIF technique, but many of the details are different. Significant effort has been devoted to (1) automatically identifying modes, especially in the presence of high noise levels, (2) developing a graphical user interface to help simplify the process of eliminating misidentified modes, and (3) developing additional techniques to help further describe the modal content, such as a discrete Fourier series decomposition and rational fraction polynomial (RFP) fitting. In general, the process is successful and relatively efficient as long as the input data is of high quality, has adequate spatial resolution to discriminate between the modes, and reference locations that are chosen to ensure that, as much as possible, they are not at nodal lines.

3.3 Energies and loss factors

The measurements required for experimental modal analysis also can be used to derive useful vibroacoustic information, such as vibrational energy and loss factors. Total loss factors (which include structural as well as sound radiation losses) using the power injection method (PIM) can be computed as

$$\eta_{total} = \text{Power Input} / (\omega \, \text{Energy}), \tag{3}$$

or using transfer functions:

$$\eta_{total} = \frac{\dfrac{P_{in}}{\left|\bar{F}\right|^2}}{\omega \dfrac{E}{\left|\bar{F}\right|^2}} = \frac{G}{\omega \tilde{E}}, \tag{4}$$

Where P_{in} is the input power, G is the conductance for a particular drive point location and $\tilde{E}$ is the Energy transfer function (energy divided by the square of the input force). These data can be extracted from the experimental measurements for each location with matching drive and response points. Another useful quantity is the acoustic radiation loss factor, which can be computed as:

$$\eta_{rad} = \frac{\frac{P_{rad}}{\left|\overline{F}\right|^2}}{\omega \frac{E}{\left|\overline{F}\right|^2}}, \tag{5}$$

where the radiated sound power P_{rad} is computed using a boundary element model of the air surrounding the panel, along with the spatial grid of measured vibration transfer functions. Here, we employ the lumped parameter BE method developed by Koopmann and Fahnline [8] to compute the radiated sound power from each mode.

Both the power injection and radiation loss factors require vibrational energy to be computed as a function of frequency. The energy can be computed directly for a given drive location i knowing the incremental structural masses at each of the response locations as

$$\tilde{E}_i = \mathbf{v}_i^H \mathbf{M} \mathbf{v}_i , \tag{6}$$

where $\mathbf{v}_i$ is a vector of mobilities (v_j/F_i) and $\mathbf{M}$ is a matrix of discretized masses at each response point j. This approach allows for the inhomogeneity of the structure to be accounted for by distributing incremental masses appropriately throughout a structure. In many previous studies in the literature, only homogenous structures are considered, so that energy is simply computed as the product of total structural mass and the spatially averaged square of velocity.

Since any measurement includes error: due to background noise, amplitude and phase calibration errors, uncertainty and error in sensor and drive location, among others, we also use the modal parameters and mode shapes to reconstruct mobility and energy functions. Once the modal parameters and mode shapes are known, the vibration response at any point j on the structure may be reconstructed as a series summation of the modes:

$$Y_{ij}(\omega) = \frac{v_j}{F_i}(\omega) \cong \sum_m \phi_{mi}(\omega)\varphi_{mj} = \sum_m \frac{i\omega}{\Lambda_m \left(\tilde{\omega}_m^2 - \omega^2\right)} f_{mi}(\omega)\varphi_{mj} , \tag{7}$$

where ϕ_{mi} are the modal response amplitudes due to a force applied at point i, φ_{mj} are the mode shapes evaluated at response point j (dimensionless, with unit amplitudes), Λ_m are the modal masses, f_{mi} are the modal forces (the products of the mode shapes evaluated at the force location i and the force amplitudes), ω is the analysis frequency, and $\tilde{\omega}_m$ are the complex resonance frequencies.

The reconstructed transfer functions may be used to compute all of the quantities described above. Also, the energies may be reconstructed more accurately, without summing over spatial distributions of velocities, by summing instead over modal energies:

$$\frac{E}{\left|\overline{F}_i\right|^2} = \sum_m \frac{E_m}{\left|\overline{F}_i\right|^2} = \sum_m \Lambda_m \phi_{mi}^2 . \tag{8}$$

Provided the modal parameters are accurate and a complete set of modes is used, the energy transfer functions should also be accurate, accounting for all inhomogenous effects (which are

captured in the modal masses), and avoiding any spatial aliasing associated with the surface integration approach in Equation 6.

The reconstructions should also filter out any background noise, as well as remove the effects of some of the measurement errors, particularly those associated with phase (which is particularly important for conductance measurements). Also, since many modal measurements are conducted using 'free' boundary conditions, where the structure is suspended from soft supports, low-frequency rigid body modes, where the structure acts as a lumped mass attached to the soft support springs, can corrupt low-frequency measurements if the suspension modes are not much lower than the structural elastic modes. By excluding rigid body modes from the reconstruction, these effects may also be removed from the transfer functions.

The reconstructed measurements should work well at low frequencies where measurement errors are most pronounced, but require that all (or nearly all) modes be included in the reconstruction. The reconstructions may not work as well at higher frequencies where it is difficult to extract all modes due to high modal overlap. At higher frequencies, therefore, it is more appropriate to use 'raw' measurements to compute energy transfer functions and conductances.

4 RESULTS

4.1 Modes and Conductance

A grid of nine points along the panel width and 14 points along the panel length was struck with the impact hammer, with six reference accelerometers mounted randomly over the surface. Some of the modal analysis results are summarized in Figure 2. The figure shows the envelope of measured conductances, along with shapes of several modes of vibration. The usual free boundary panel mode patterns are evident, and are classified by mode orders (m, n), where m indicates the mode order given by the number of node lines (regions of near 0 vibration) along the length, and n indicates the mode order along the width.

Figure 3 compares the shaker-based conductance measurements to those measured using the impact hammer and reference accelerometer approach. The shaker-based and raw hammer-based conductance measurements are corrupted by phase errors (where conductance becomes negative, which is physically impossible) and scalloping caused by the boxcar window applied to the measurements. The hammer and accelerometer based conductance errors are also corrupted by differences between the locations of the driven points and the adjacent accelerometers (since the accelerometer locations cannot be struck directly). To remove these effects, the conductance is reconstructed using the extracted modes. The reconstructed conductance is also shown in Figure 3, and agrees well with the high frequency conductances, while exhibiting a smooth, accurate low frequency character. All high frequency conductance estimates also agree well with an analytic conductance estimate [1], which exhibits the well-known high frequency 'tail-up' caused by the transition of flexural waves to pure shear waves in stiff lightweight sandwich panels with low core shear moduli.

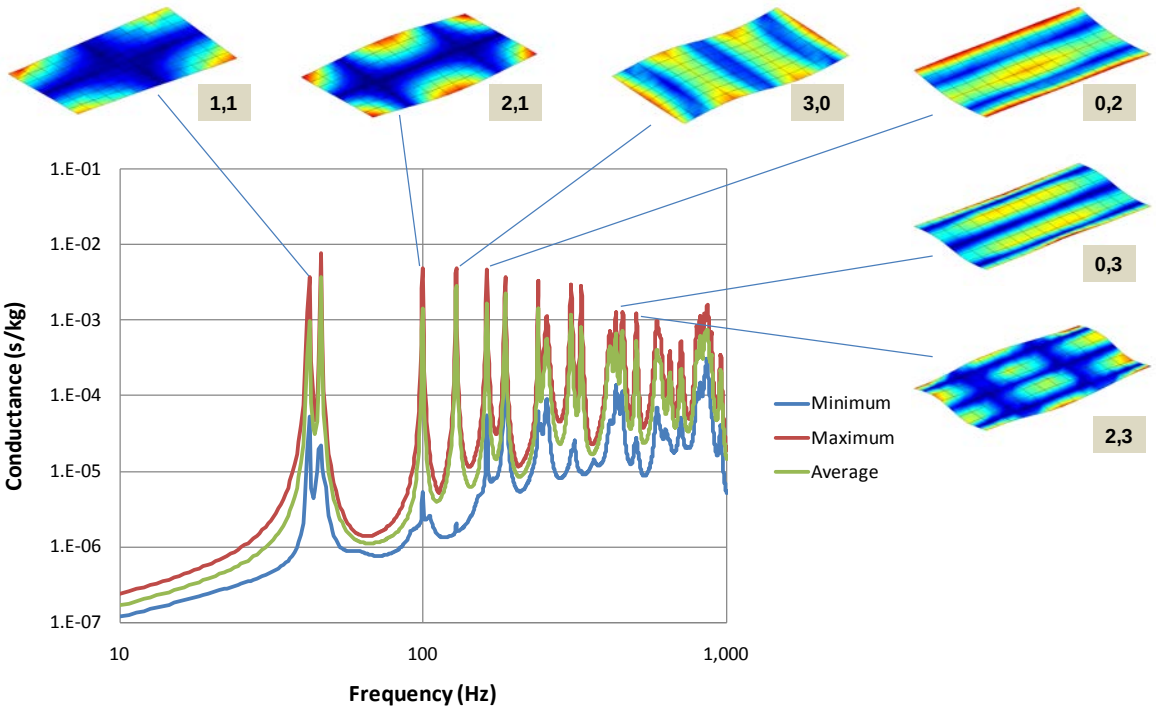

Figure 2: Sandwich panel conductance (showing envelope of measurements) and low frequency modes.

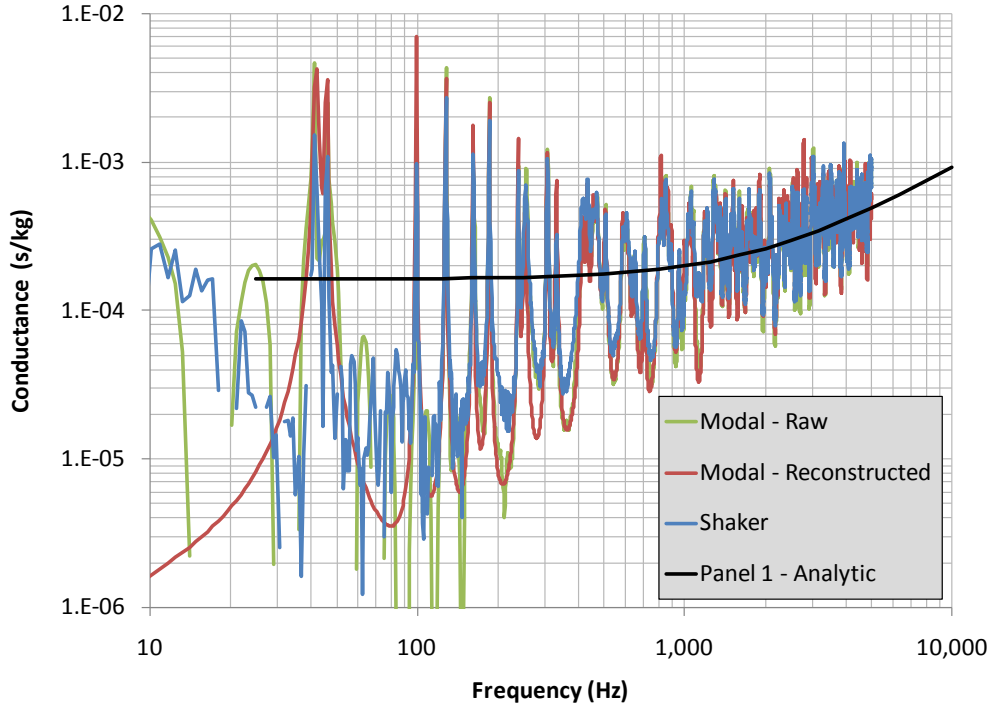

Figure 3: Measured conductance using shaker and modal (hammer) data.

4.2 Energies

Energies (actually Energy/Force^2 transfer functions) were estimated in three ways: (1) by averaging normal velocity/force transfer functions over a randomly positioned array of six accelerometers for each of six randomly positioned shaker drives, (2) by averaging normal transfer functions between each impact hammer drive and reference accelerometer (14x9 arrays), and (3) by summing modal energies using Equation 8 for each reference accelerometer location. These data were then averaged for each drive location to produce the overall panel averaged energy transfer functions.

The raw and modal-based energy transfer functions (based on the surface averaging in method 2) are shown in Figure 4. Raw data, along with data reconstructed based on the RFP extracted modes are shown. At low frequencies, the raw energies are biased slightly high due to measurement error, or the effects of rigid body suspension modes. Above 100 Hz, however, the raw and reconstructed energies are nearly identical.

Figure 5, however, compares the energy transfer functions reconstructed based on surface averaging, as well as summing over modal energies (method 3), and shows that the surface averages are higher than the modal energy-based energies. We will revisit this discrepancy when we examine loss factors. Comparing loss factors based on power injection methods to those extracted from the modal analysis will allow us to determine which of the energy transfer function estimates is correct.

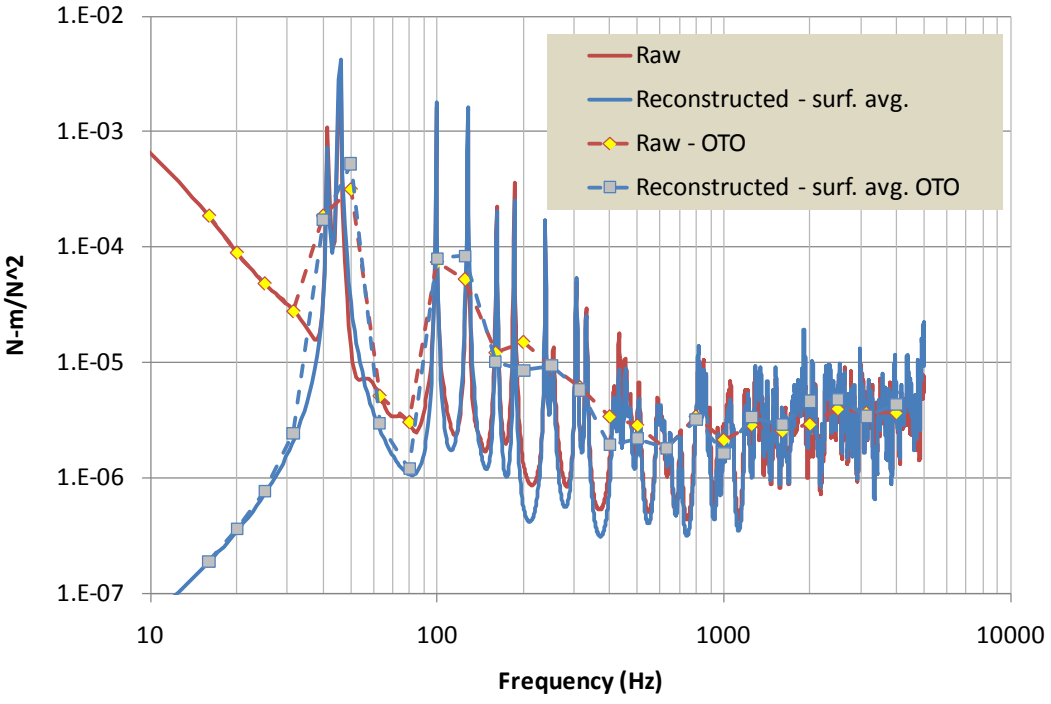

Figure 4: Raw and reconstructed measured modal energy transfer functions.

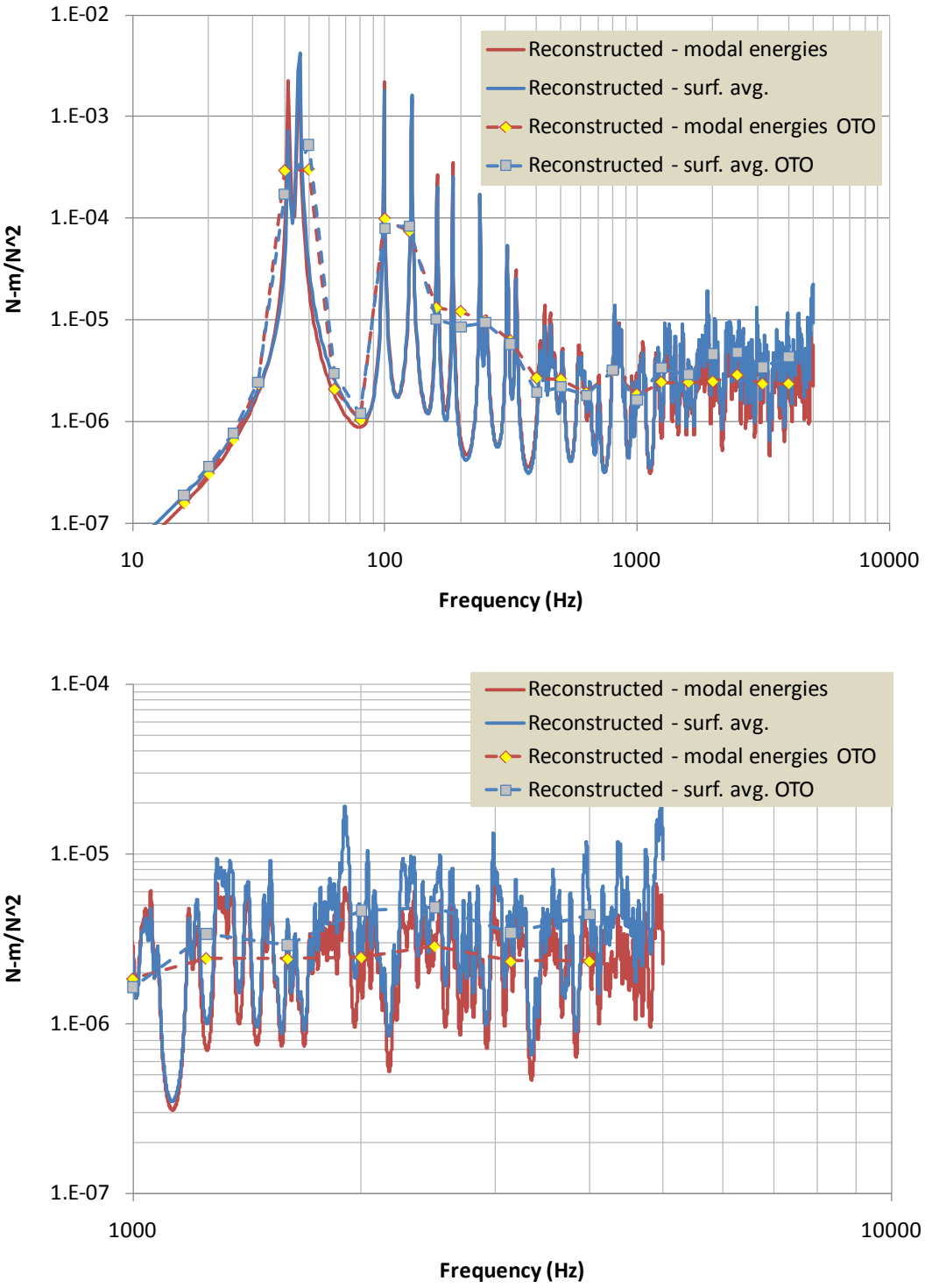

Figure 5: Energy transfer functions reconstructed based on modal energies and surface averages. Top – overall; bottom – zoomed to high frequencies.

4.3 Structural and Radiation Damping

The conductances and energy transfer functions are used to compute loss factors using the Power Injection Method. The modal loss factors are used to establish the accuracy of the measured energy transfer functions by comparing them to the PIM-based loss factors in Figure 6. PIM loss factors computed using modally reconstructed energies (using both surface averaging and modal energies), as well as the six accelerometer average from the shaker data are shown in the Figures. The PIM loss factors based on the modal energies agree very well with the modal loss factors. The shaker-data based loss factors, however, are biased high at low frequencies (since the 6-accelerometer based energies are biased low due to neglecting the additional energy at the heavier panel ends) and biased low at high frequencies. The loss factors based on modally reconstructed surface-averaged energies are also biased low. The high frequency bias indicates that the shaker-based and surface-averaged energies are clearly too high above 2 kHz, due to spatial aliasing of the vibration fields. Figure 6 also includes loss factors measured using the decay method, where the panel is struck with an impact hammer and the time histories of the accelerometers are used to determine decay rates over one-third octave bands. The decay rate loss factors provide an additional useful confirmation of the accuracy of the modal and PIM (based on modal energy) loss factors.

The modal and PIM loss factors show strong peaks centered at about 500 Hz, which is near the critical frequency of the panels. The character of the loss factor curves resembles that of typical radiation loss factors. To establish the impact of radiation damping on the overall panel damping, a BE analysis of the radiated sound power from the panel modes was conducted, and the radiation loss factors computed using Equation 5. The radiation loss factors are compared to the modal loss factors in Figure 7 and clearly dominate the panel loss factors for frequencies up to 1 kHz. Above 1 kHz, the radiation loss factors diminish, so that the panel loss factors are dominated by internal structural damping at high frequencies, which appears to be about 0.007 over all frequencies.

5 CONCLUSIONS

Conductance, energy, and damping loss factors are computed for a sandwich panel using several methods, including traditional shaker and accelerometer averaging, as well as experimental modal analysis. The modal analysis approach allows reconstruction of FRFs, conductances, and energy transfer functions, filtering out experimental errors. Energies based on modal parameters are more accurate than those computed using surface-averaging, which are biased high with increasing frequency. Radiation damping is pronounced in stiff lightweight sandwich panels, and is computed by applying an acoustic BE model to the vibration fields. The acoustic boundary element method may be used to routinely compute radiation damping for a structure. The radiation damping may then be subtracted from total damping measurements to produce structural-only (in-vacuo) damping estimates.

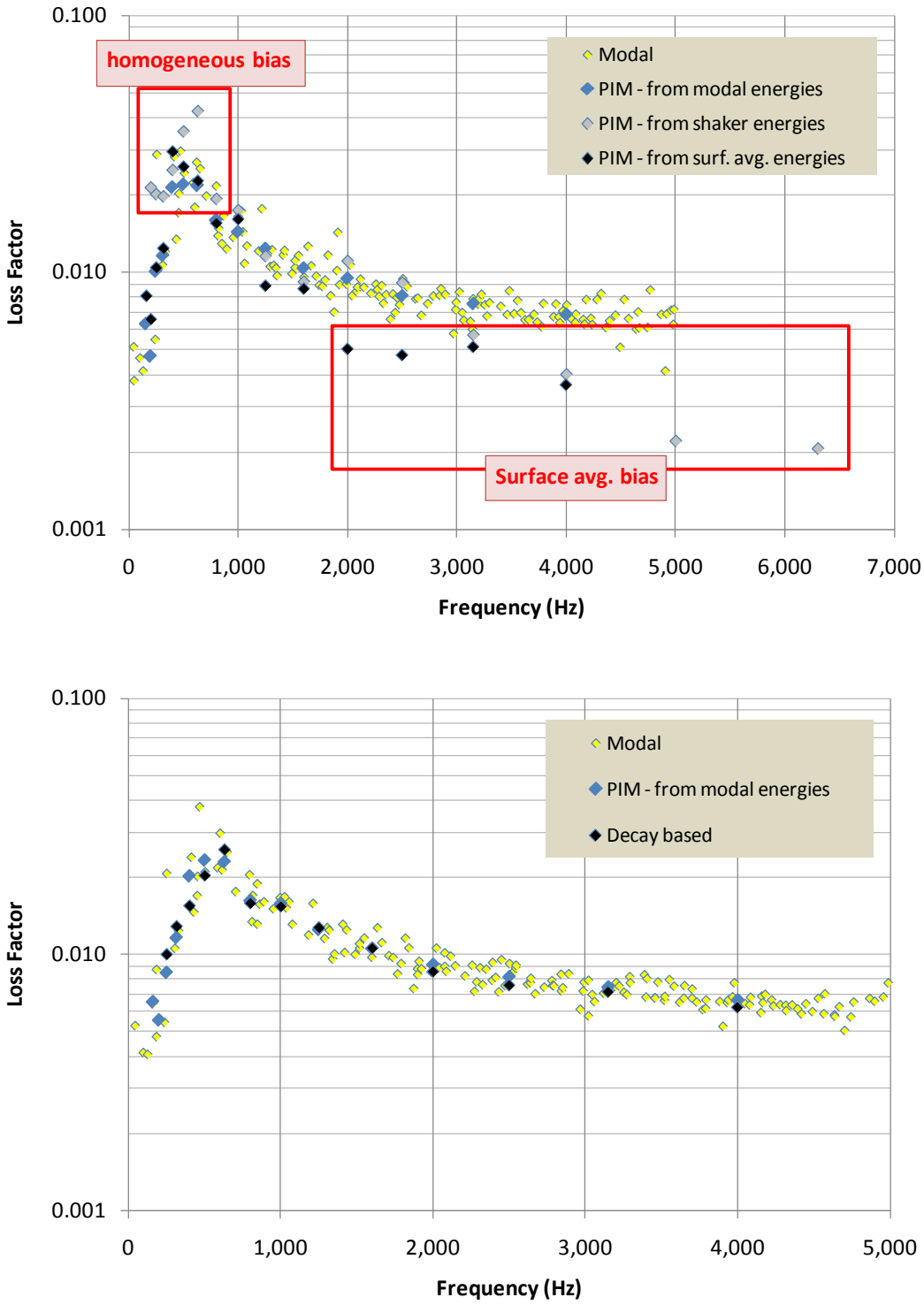

Figure 6: Modal and one-third octave loss factors. Top – modal vs. power injection method (PIM) using various energies; Bottom – modal vs. PIM vs. decay based measurements.

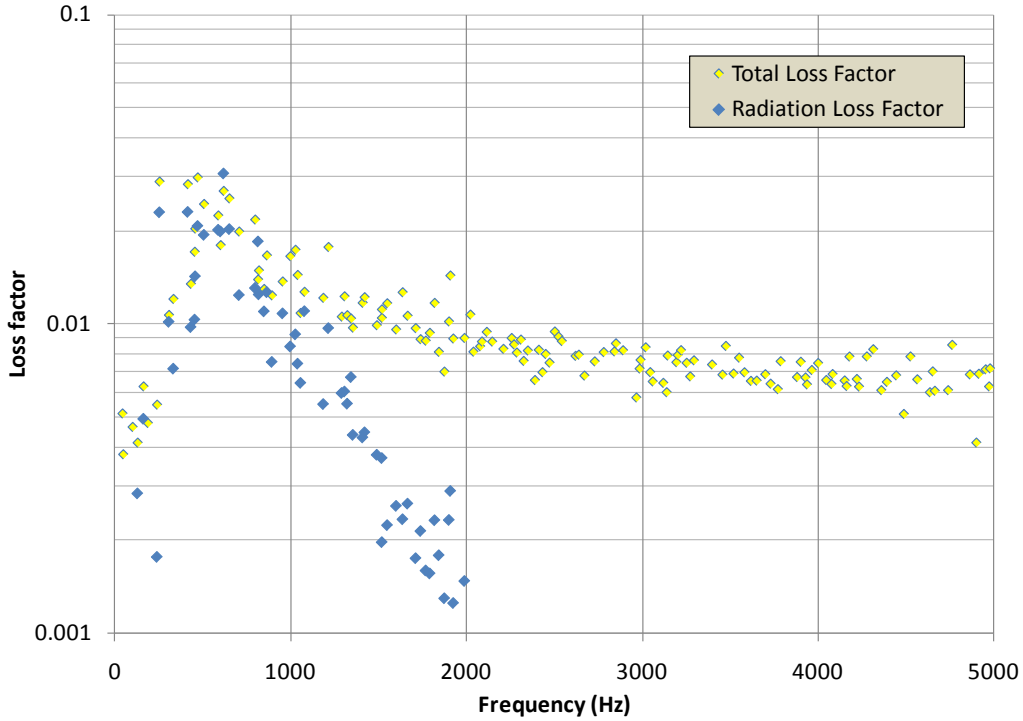

Figure 7: Total and radiation modal loss factors.

REFERENCES

[1] S.A. Hambric, S.C. Conlon, B.G. Grisso, and M.R. Shepherd. Measurements of the power flow between bolted honeycomb sandwich panels. *Internoise 2009*, Ottawa, Canada, 23-26 August 2009.

[2] S.A. Hambric, A.R. Barnard, and S.C. Conlon. Power transmission coefficients based on wavenumber processing of experimental modal analysis data for bolted honeycomb sandwich panels. *Internoise 2010*, Lisbon, Portugal, 13-16 June 2010.

[3] C.Y. Shih, Y.G. Tsuei, R.J. Allemang, and D.L. Brown. Complex mode indication function and its applications to spatial domain parameter estimation. *Proceedings of the Seventh International Modal Analysis Conference*, pp. 533-540, 1989.

[4] A.W. Phillips, R.J. Allemang, and W.A. Fladung. The complex mode indication function (CMIF) as a parameter estimation method. *Proceedings of the Sixteenth International Modal Analysis Conference*, pp. 705-710, 1998.

[5] S. Li, W.A. Fladung, W.A. Phillips, and D.L. Brown. Automotive applications of the enhanced mode indicator function parameter estimation method. *Proceedings of the Sixteenth International Modal Analysis Conference*, pp. 36-44, 1998.

[6] F. Necati Catbas, D.L. Brown, and A. Emin Aktan. Parameter estimation for multiple-input multiple-output modal analysis of large structures. *J. Eng. Mech.*, **130** (8), pp. 921-930, 2004.

[7] J.B. Fahnline. Computing fluid-coupled resonance frequencies, mode shapes, and damping loss factors using the singular value decomposition. *JASA*, **115** (4), pp. 1474-1482, April 2004.

[8] G.H. Koopmann and J.B. Fahnline. *Designing Quiet Structures*. Academic Press, 1997.